Classical molecular dynamics simulations of behavior of GeO_2 under high pressures and at high temperatures

K. V. Shanavas, Nandini Garg, and Surinder M. Sharma
Synchrotron Radiation Section, Bhabha Atomic Research Centre, Mumbai 400085, India
(Received 17 November 2005; revised manuscript received 18 January 2006; published 23 March 2006)

We have investigated the high-pressure and high-temperature behavior of GeO_2 with the help of extensive molecular dynamics simulations. Our calculations show that α-GeO_2 transforms reversibly to a denser and higher-coordinated (Ge-O) monoclinic phase at ~8 GPa, reasonably close to the experimental observation of 7.8 GPa. Our simulations on vitreous GeO_2 show that, at higher pressures, substantial numbers of Ge atoms are coordinated with five oxygen atoms. However, our results do not support the existence of an entirely pentahedrally coordinated state, claimed to have been observed recently. The simulations on the liquid phase, carried out at several temperatures, display the existence of a first-order phase transition under compression. Our results suggest that this may not be a low-density to high-density liquid-liquid transformation as the denser phase is found to be solidlike. These results suggest the necessity of a more careful characterization of the high pressure phase obtained from compression of the liquid phase in the experiments.

DOI: 10.1103/PhysRevB.73.094120 PACS number(s): 61.20.Ja, 64.70.−p, 02.70.Ns, 61.43.Fs

I. INTRODUCTION

Silica is one of the most widely studied materials due to its geophysical importance. Several similarities with SiO_2 have prompted numerous investigations on GeO_2 as well. In particular, the comparison of various structural aspects of these compounds suggest GeO_2 to be a high-pressure analog of SiO_2, giving rise to the possibilities of seeing similar changes under less severe thermodynamic conditions.[1,2]

The phase diagram of GeO_2 shows several structural changes.[3] The stable phase at ambient conditions is of rutile type, in which the Ge-O are octahedrally coordinated. On increasing the temperature, the rutile phase transforms to the tetrahedrally coordinated α-quartz phase around 1280 K. Due to the sluggish nature of the α to rutile transformation on decrease of temperature, the quartz phase can be quenched metastably at ambient conditions. The α phase when heated transforms to the β phase[4] above 1020 K and eventually melts at 1378 K to form a network-structured liquid. Recent experiments[5] have shown that at elevated temperatures and pressures GeO_2 undergoes several phase transformations, such as the rutile to $CaCl_2$ type followed by α-PbO_2 type and then to pyrite type. Recent x-ray diffraction experiments have shown that at room temperatures α-GeO_2 transforms to a poorly crystallized distorted rutile-type $P2_1/c$ monoclinic structure above 6 GPa,[6,7] at variance with several earlier studies suggesting amorphization.[8] At room temperatures, earlier x-ray absorption measurements[1] were interpreted to imply that in α-GeO_2, Ge-O coordination increases irreversibly from fourfold to sixfold between 7 and 9 GPa. The α to rutile structural change in the single-crystalline sample was found to be irreversible, diffusive on heating, and displacive under compression at room temperatures.[7]

Like silica glass, amorphous GeO_2 has also been shown to undergo low-density amorphous to high-density amorphous phase transformation.[1,2,9–12] The observed pressure-induced variations in the x-ray absorption near-edge structure indicated that the evolution of the measured Ge-O distances can be interpreted in terms of two distinctly coordinated sites rather than a progressive site modification.[1] From Raman scattering intensity measurements Polsky *et al.*[2] have shown that a structural relaxation process associated with the gradual coordination increase from 4 to 6 proceeds through the creation of an intermediate five-coordinated metal species in these glasses. Recent *in situ* x-ray and neutron diffraction measurements[13] on GeO_2 have shown transformation to a dense octahedral glass below 15 GPa. A metastable, intermediate phase with constant average Ge-O coordination of ~5 was also observed between 6 and 10 GPa.

In the last few years, the existence of pressure-induced, first-order, low to high density, liquid-liquid phase transitions has attracted a lot of attention. Liquid polymorphism has been observed in various experiments[14–17] and computer simulations.[18–21] In particular, the liquids that have tetrahedral molecular bonding, such as Si, Ge, C, SiO_2, and GeO_2, have been shown to undergo pressure-induced polymorphism.[22] Recent *in situ* x-ray absorption measurements by Ohtaka *et al.*[23] on liquid alkali-metal germanates have shown a sharp coordination change in the pressure range 2.5–4 GPa. Experiments were carried out on alkali-metal germanate (composition Li_2O-$4GeO_2$ with B_2O_3 as an additive) rather than pure germania to lower the melting temperature and to suppress the decomposition of GeO_2. (These experiments were carried out at ~1273 K, i.e., below the melting point of germania.) In particular, the deduced Ge-O bond distances exhibited a sharp increase in the pressure range mentioned above and monotonically decreased thereafter.

High-pressure behavior of germania has also been investigated with the help of molecular dynamics (MD) simulations.[24–29] Simulations by Tsuchiya *et al.*[24,26] carried out with a MD cell containing 300 Ge and 600 oxygen atoms showed that the amorphization of α-GeO_2 at ~7 GPa is associated with a mechanical instability. These studies also showed that α-GeO_2 transforms to the rutile phase under the

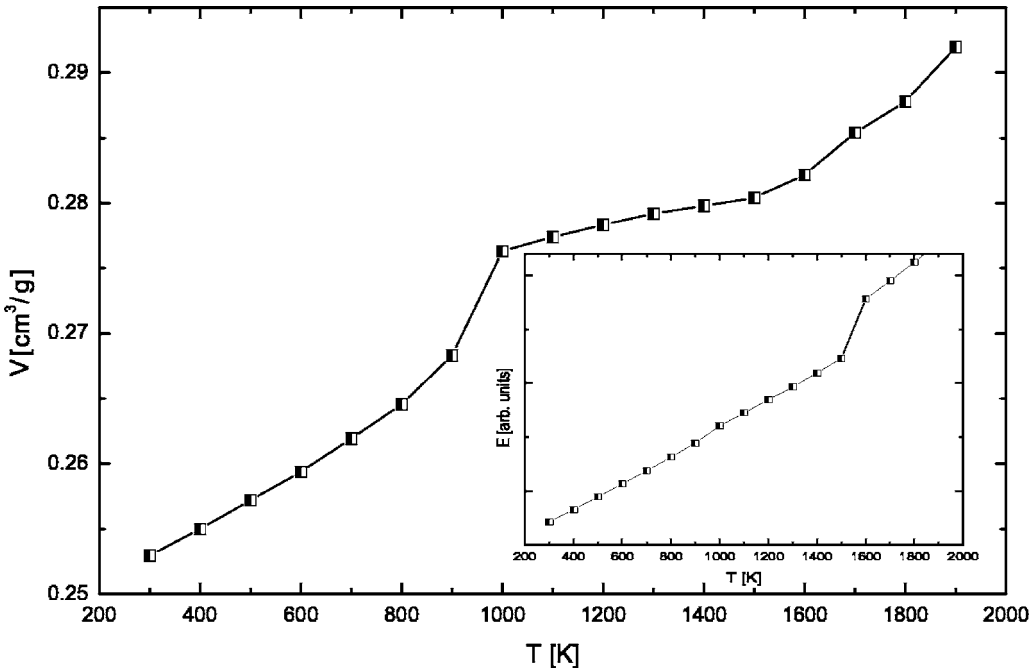

FIG. 1. Variation of volume with temperature of α-GeO_2 at ambient pressure. Inset shows the variation of enthalpy with temperature.

presence of shear stress. With the help of *ab initio* calculations, Oeffner and Elliot[4] have generated reliable pair potentials for GeO_2 which reproduce the α and rutile phases as well as the vibrational density of states. Recently, using these potentials, Gutiérrez and Rogan have simulated the behavior of GeO_2 at high temperatures.[25] A small volume collapse observed in their calculations (with constant *NVE*, i.e., a micro-canonical ensemble, with a box of 576 particles) was interpreted to imply the possibility of liquid-liquid transformation between 4 and 8 GPa. Similar (constant *NVE*) simulations on vitreous GeO_2 have also been carried by Micoulaut[28] using potentials of Oeffner and Elliot,[4] modified to include steric repulsion and electronic polarizability of ions. These simulations, carried out on a cell having 768 atoms, showed that pressure brings about an irreversible (stepwise) increase in the average Ge-O coordination. However, this increase in the Ge-O coordination was explained in terms of an average of four- and six-coordinated states, as also proposed by Itie *et al.*[1] Still another simulation, using the pair potentials of Refs. 24 and 26, explained the temperature-induced densification of vitreous GeO_2 in terms of rigidity percolation brought by an increase in the coordination number around 0.5 GPa. This simulation, though carried out only at a few pressures, also suggests that under compression Ge-O coordination increases.

In the present paper, we present our results of extensive classical molecular dynamics simulations on GeO_2 with the pair potentials of Oeffner and Elliot.[4] In contrast to earlier simulations, we use the rescaled potentials, which are known to reproduce the vibrational density of states of quartz as well as rutile phases of GeO_2 rather well. In particular, the results of the following simulations are presented: (i) behavior of α-GeO_2 at high temperatures; (ii) high- pressure study of α-GeO_2; (iii) high-pressure study of vitreous GeO_2; and (iv) high-pressure study of liquid GeO_2. Of these, the behavior of α-GeO_2 at high temperatures is studied to test the reliability of the simulations and also to determine the melting temperature.

II. COMPUTATIONAL PROCEDURE

Molecular dynamics simulations are carried out on a macrocell of 4374 atoms (1458 Ge+2916 O) using DL_POLY,[30] employing the Nosé-Hoover *NPT* ensemble with the variable cell method and periodic boundary conditions. Usage of a larger number of atoms in this simulation should help obtain more reliable results for the vitreous and liquid state than the earlier simulations. The Verlet leapfrog integration algorithm is used with a time step of 2.0 fs. Typical relaxation times for the thermostat and barostat are taken as 5.0 and 10.0 ps, respectively. In addition, for a smoother evolution to the new thermodynamic state, velocity is scaled every few hundred time steps in the initial stages. Fluctuations in the macroscopic physical quantities like total energy, cell volume, etc. are monitored to ascertain equilibration. Typically, each configuration is equilibrated for about 100 ps before averaging. However, close to the phase transitions equilibration is found to be slow and hence the states were equilibrated for $\sim$250–300 ps.

As mentioned above, for our simulations we used the rescaled interatomic interaction potential of Oeffner and Elliot.[4]

TABLE I. Interaction pair potential parameters used in MD simulations.

	A_{ij} (kJ/mol)	ρ_{ij} (Å)	C_{ij} (kJ Å^6/mol)
Ge-O	7.9108×10^6	0.16315	9000
O-O	2.9259×10^5	0.304404	4985
Effective charge	$Z_{Ge}=-2Z_O=0.941\,74e$		

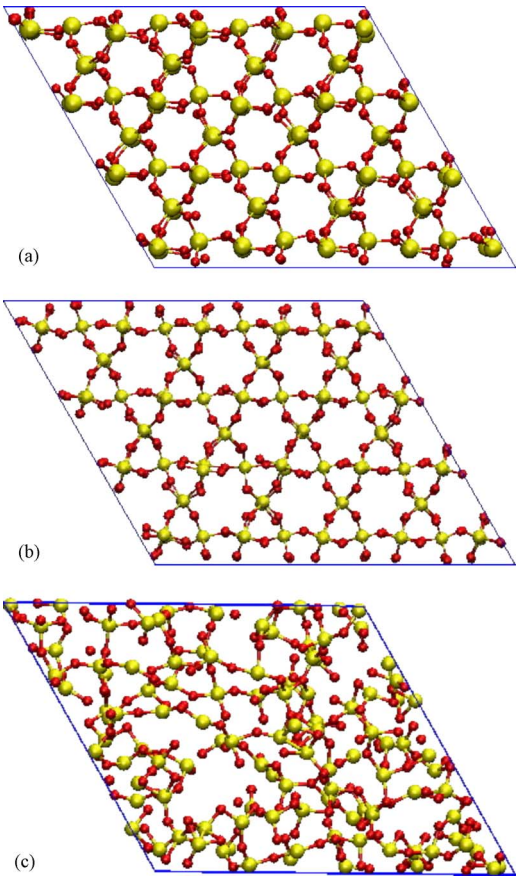

FIG. 2. (Color online) Simulated structure of GeO_2 (a) at 300 K (α-quartz), (b) at 1200 K (β-quartz), and (c) at 1800 K. Only a few atoms close to the center of the MD cell, as viewed down the c axis of the MD cell (parallel to the c axis of α-GeO_2), are shown.

These pair potentials have the Buckingham form, i.e.,

$$V(r_{ij}) = \frac{q_i q_j}{r_{ij}} + A_{ij}\exp(-r_{ij}/\rho_{ij}) - \frac{C_{ij}}{r_{ij}^6}.$$

Relevant parameters of the potential are given in Table I.

For our simulations, the initial atomic positions in the macrocell are generated from the experimentally known positional coordinates of atoms in the α-quartz phase.[31] High-temperature behavior of α-GeO_2 is investigated by raising the temperature of the equilibrated quartz structure up to 2000 K, in steps of 100 K, allowing equilibration for about 100 ps at each temperature. The liquid phase was generated by heating the α phase to 3500 K and then cooling the equilibrated structure to 3000 K and subsequently to 2000, 1650, and 1500 K at a rate of 5 K/ps. To generate the glass, the equilibrated liquid at 2000 K was cooled below its melting point to 1200 and 300 K at a rate of 5 K/ps. At all final temperatures the system was allowed to equilibrate for sufficient time (~200–300 ps) before increasing the pressure. To investigate the effects of compression, pressure was in most cases raised in steps of 1 GPa. Equilibrium properties like bond lengths, coordination number, etc. were calculated averaging over 1000 configurations. As discussed later, the differences between liquid and solid phase were evaluated in terms of shear rigidity and diffusion.

Once the coordinates in the simulated structures are known several observable quantities can be computed from these. For example, the radial distribution functions or pair-correlation functions $g_{\alpha,\beta}(r)$ between two types of atoms α and β are calculated by considering spherical shells of thickness Δr around the atom α and then counting the number of

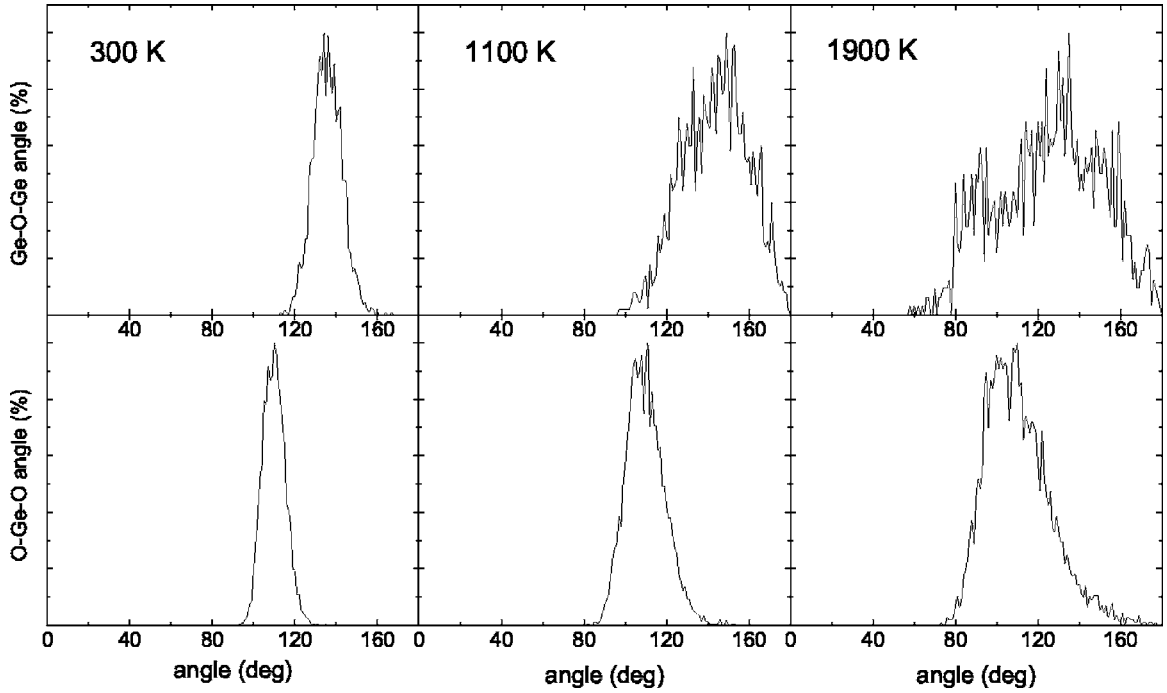

FIG. 3. Ge-O-Ge and O-Ge-O angle distribution at different temperatures. Ge-O-Ge peak shifted from 135° in the α phase to about 145° in the β phase. O-Ge-O angle does not change its position, suggesting that the tetrahedra are preserved.

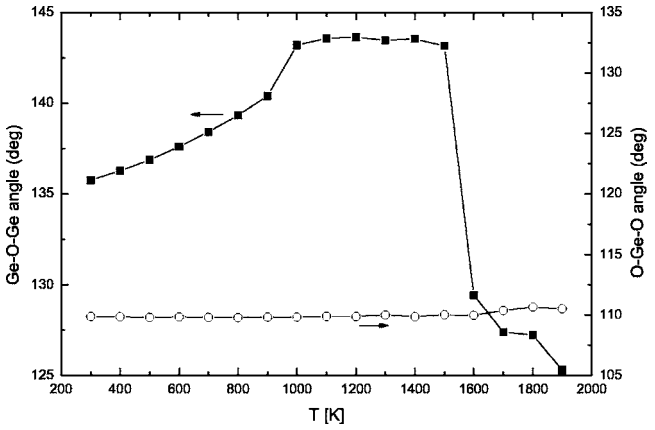

FIG. 4. The variation of average Ge-O-Ge and O-Ge-O bond angles with temperature at ambient pressure. The fact that the Ge-O-Ge angle varies while the O-Ge-O angle remains more or less constant suggests that the transformations are brought about by the spatial rearrangement of tetrahedra.

atoms of type β in the shell. The corresponding probability is given by the relation

$$\langle n_\alpha(r) n_\beta(r+\Delta r)\rangle = \rho_\beta 4\pi r^2 g_{\alpha\beta}(r)\Delta r.$$

Partial structure factors are calculated by Fourier transforming the corresponding partial pair correlation function, as

$$S_{\alpha\beta}(k) = \delta_{\alpha\beta} + 4\pi\rho(c_\alpha c_\beta)^{1/2} \times \int_0^R r^2[g_{\alpha\beta}(r) - 1]\frac{\sin(kr)}{kr} W(r)dr,$$

where $c_\alpha = N_\alpha/N$ is the concentration of α species. The window function $W(r) = \sin(\pi r/R)/(\pi r/R)$ is used to reduce termination effects and R is generally chosen to be about half of the simulation cell.

III. RESULTS AND DISCUSSION

A. α-GeO_2 at high temperatures

Figure 1 shows the computed variation of the volume ($1/\rho$ cm^3/g) of α-GeO_2 with temperature. The results show that between 900 and 1000 K, the slope of variation increases substantially (density drop of ~2.9% across 100 K) followed by a reduction in the slope beyond 1000 K. On further increase in the temperature, the slope increases again at ~1500 K. The inset in Fig. 1 shows the variation of enthalpy of the system[32] with temperature, displaying a continuous variation at ~1000 K but an abrupt increase at ~1500 K. This suggests that structural changes at ~1000 K are not as dramatic as at ~1500 K. Figure 2 shows the structures at ambient conditions, 1200 K, and 1800 K. The structure at 1200 K is obviously crystalline and closely related to that of the α phase except that the threefold axis is now sixfold. This is typical of the $\alpha \rightarrow \beta$ transition. However the structure at ~1800 K is quite disordered. To gain more insight into the nature of changes, we present in Figs. 3 and 4 the associated variations in the related structural parameters.

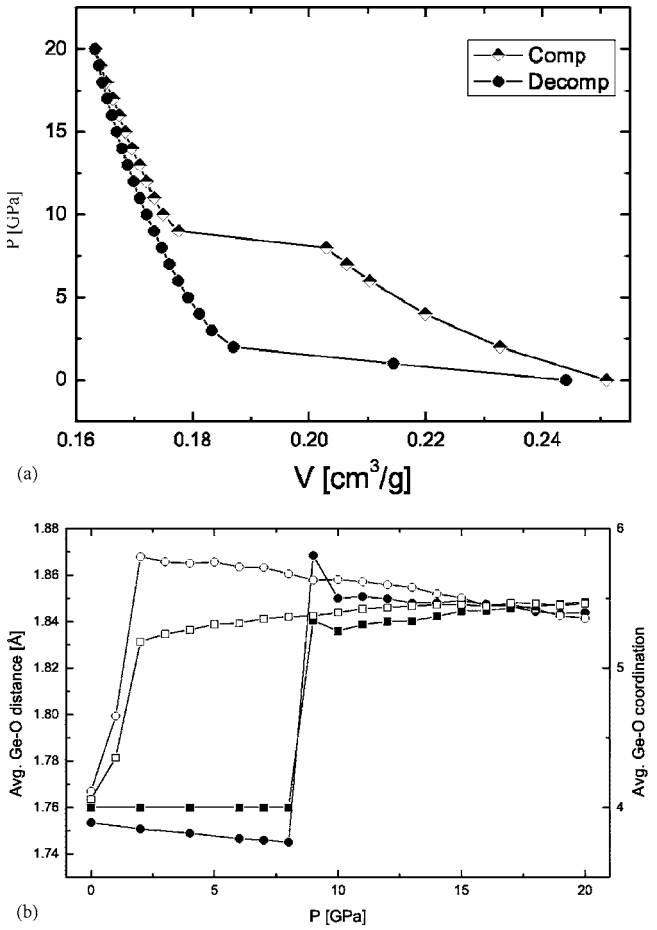

FIG. 5. (a) Computed variation of volume with pressure for α-GeO_2. (b) Calculated variations of Ge-O distance and coordination with pressure for α-GeO_2. Solid squares represent the Ge-O coordination with increasing pressure while unfilled ones represent the behavior on release of pressure. Corresponding variation of Ge-O distance is represented by the circles.

Temperature-induced variations of intratetrahedral (O-Ge-O) and intertetrahedral (Ge-O-Ge) angles are shown in Figs. 3 and 4. The O-Ge-O bond angle, originally peaked around 109°, broadened on increase in the temperature, but showed no discontinuous changes at ~1000 and ~1500 K. However, the intertetrahedral Ge-O-Ge angle showed an increase of ~3° at ~1000 K and broadens significantly at temperatures higher than 1500 K. These results, coupled with the fact that no discontinuous change is observed in Ge-O, Ge-Ge, and O-O distances, imply the integrity of the tetrahedra in the α to β transition. The temperature of transformation for this structural change is reasonably close to the experimental value of 1020 K as quoted by Oeffner and Elliot Essentially this transformation is brought about by a cooperative spatial rearrangement of tetrahedra, as in similar transitions in quartz (SiO_2).[33–35]

The broadening of the computed Ge-O-Ge bond angle distribution beyond 1500 K represents the random orientations of tetrahedra, which could result in the breakdown of long-range order. The related sudden increase in the enthalpy (inset Fig. 1) suggests that the disordered structure beyond 1500 K, as shown in Fig. 2(c), may be the liquid state (the

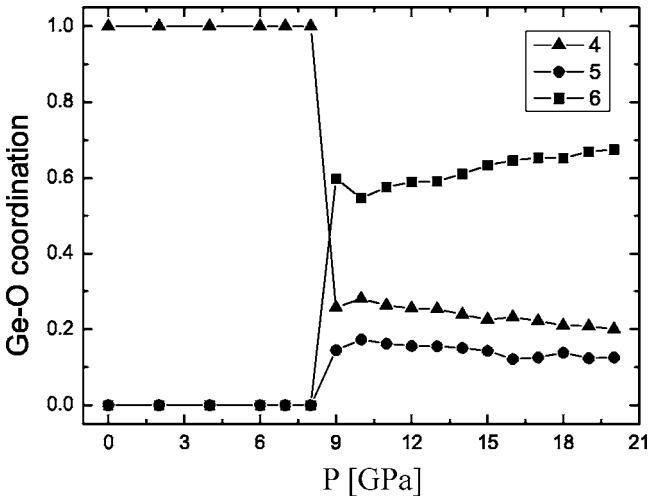

FIG. 6. Pressure-induced variation of fraction of Ge atoms having four, five, and six coordination with oxygen atoms in α-GeO_2.

experimental melting temperature of GeO_2 is 1378 K). The existence of the liquid state is further supported by the following simulation. The atomic coordinates of the MD cell were so shifted that the MD cell deformed[36] by an angle of about 2°, and then the state was equilibrated. The cell remained deformed as in the initial state even after equilibration of several picoseconds. In contrast, at 1200 K, it transforms back to the undeformed state. To characterize the state in terms of network connectivity between the polyhedra (tetrahedra/octahedra), the numbers of oxygen ions shared by different germanium ions were counted. We found that below the melting temperature all the tetrahedra are corner linked. However, in the molten phase, apart from the corner-linked tetrahedra we also find a small percentage ($<10\%$) of edge-shared tetrahedra as also observed by Gutiérrez and Rogan.[25] In fact the sharp decrease in the average Ge-O-Ge angle at $\sim$1500 K shown in Fig. 4 is due to the change in connectivity in the melt. The smaller average Ge-O-Ge angle for temperatures higher than 1500 K is also consistent with the earlier calculations of Ref. 25

The simulations presented in this section reproduce well the experimental observations of the transformations to the β phase and the melting, thereby implying that the potentials used here are reasonable for evaluating the structural changes with temperature.

B. α-GeO_2 under high pressures

Before we discuss the behavior of amorphous phase at high pressures and temperatures, we will present here the results of our simulations on the high-pressure behavior of α-GeO_2. Figure 5(a) shows that the α-GeO_2 undergoes a first-order phase transformation at $\sim$8 GPa to a denser phase ($\Delta V/V \sim 10\%$). On decompression from 30 GPa, the denser phase transforms back to a lower-density phase at $\sim$2 GPa. Associated variations in the Ge-O distance and the average Ge-O coordination are shown in Fig. 5(b). We note that the Ge-O distance decreases up to $\sim$8 GPa followed by a steep jump at 9 GPa and a decrease again beyond this pressure.

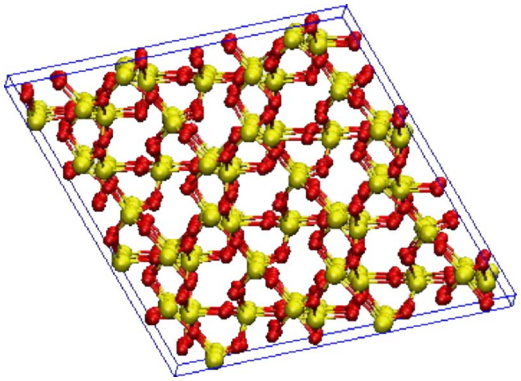

FIG. 7. (Color online) Simulated high-pressure phase of GeO_2 at 9 GPa.

These pressure-induced changes are associated with the concomitant changes in the average Ge-O coordination. However, the phase at high pressure is not fully six coordinated and the Ge-O coordination approaches $\sim$5.6 at $\sim$20 GPa. Figure 6 shows that the structure at $\sim$9 GPa has ($\sim$15%) Ge atoms with five (Ge-O) coordination, in addition to the atoms having four and six coordination. These results are similar to the results of earlier MD simulations on SiO_2.[37]

On release of pressure the average Ge-O bond length as well as coordination revert back to almost the initial values. These results are at slight variance with the conclusions drawn by Itie *et al.*[1] from their extended x-ray absorption fine-structure (EXAFS) measurements. Though it is possible that the relaxation mechanism is more impeded in real physical systems than in computer simulations, it may still be interesting to verify the results of our simulations with more precise measurements and analysis in terms of states of mixed coordination. The structure of GeO_2 at 9 GPa is shown in Fig. 7. The equilibrated macrocell shape at $\sim$9 GPa is monoclinic. The main features of the computed diffraction pattern of the daughter phase compare well with the experimental diffraction pattern of Haines *et al.*[6] The radial distribution function of this phase, shown in Fig. 8, indicates (when compared to Fig. 9 of the amorphous phase)

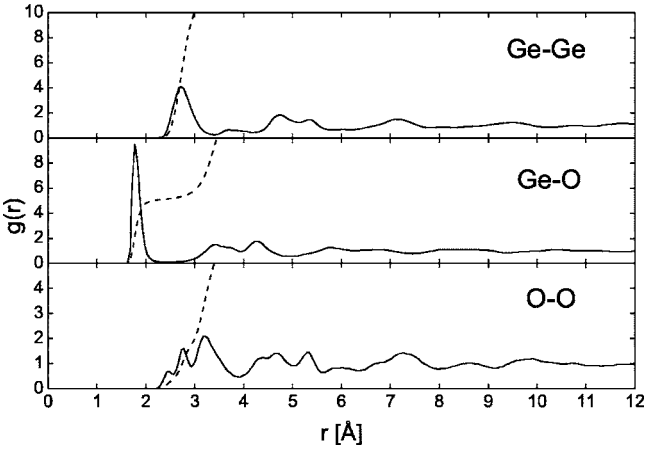

FIG. 8. Radial distribution functions for the high-pressure phase of α-quartz at 9 GPa. Dotted line represents the running coordination number.

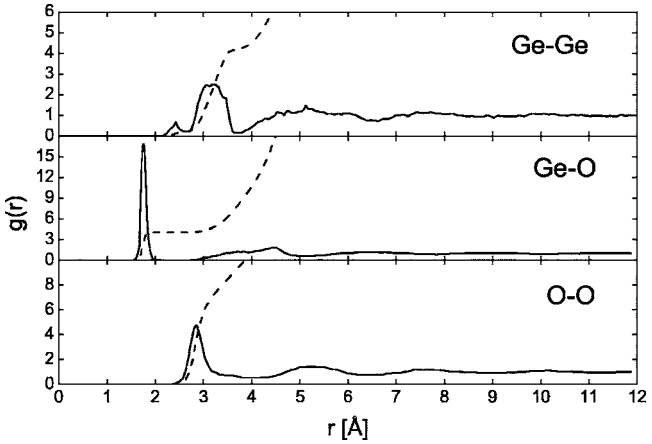

FIG. 9. Partial radial distribution functions for vitreous GeO_2 at ambient conditions. Dotted line represents the running coordination number.

that the new phase retains crystallinity and is not amorphous as claimed in earlier simulations.[38] This phase was found to be stable and did not transform to a rutilelike phase upon heating.

A separate simulation on β quartz at 1200 K shows that it too undergoes a first-order phase transition to a disordered octahedral structure around 6 GPa. The structure mainly contained edge-shared octahedra, unlike the rutile phase. As there are no reported experimental studies on β-GeO_2, these results are not presented here.

C. High-pressure study of vitreous GeO_2

At ambient pressure, the simulated glassy structures correspond to the densities of 3.98 and 3.65 g/cm^3 at 300 and 1200 K, respectively. The analyses of the simulated structures of vitreous GeO_2, in terms of the radial distribution function, partial structure factors, and distributions of O-Ge-O and Ge-O-Ge angles show that at 300 and 1200 K the structures are essentially similar. For the amorphous structure at 300 K, the partial radial distribution functions are shown in Fig. 9. Here we should note that as 3.65 g/cm^3 is the density of GeO_2 at 1200 K (i.e., the solid phase), the simulations carried out by Gutierréz *et al.*[25] at this and higher densities are unlikely to represent liquid simulations.

The sharp peak and relatively flat running coordination number at 4 in the Ge-O correlation function means that *almost* the entire structure is made of interconnected tetrahedra. In fact, the direct counting of network connectivity revealed that 99.7% of the structural units are tetrahedra and of these 92% are corner linked. Corresponding partial structure factors $S_{\alpha\beta}(k)$ are shown in Figs. 10(a) and 10(b) summarizes the computed changes in the structure factor with pressure for vitreous GeO_2. The principal features are peaks occurring at $\mathbf{k}=1.81$ (the first sharp diffraction peak), 2.65, and 4.5 Å^{-1}, which compare well with the results of Gutierréz *et al.*[25] and Micoulaut.[28] In addition, it is very reassuring to note that the experimental results, the structure factor computed by us, and earlier MD results using modified potentials,[28] as well as the structure factor computed with the

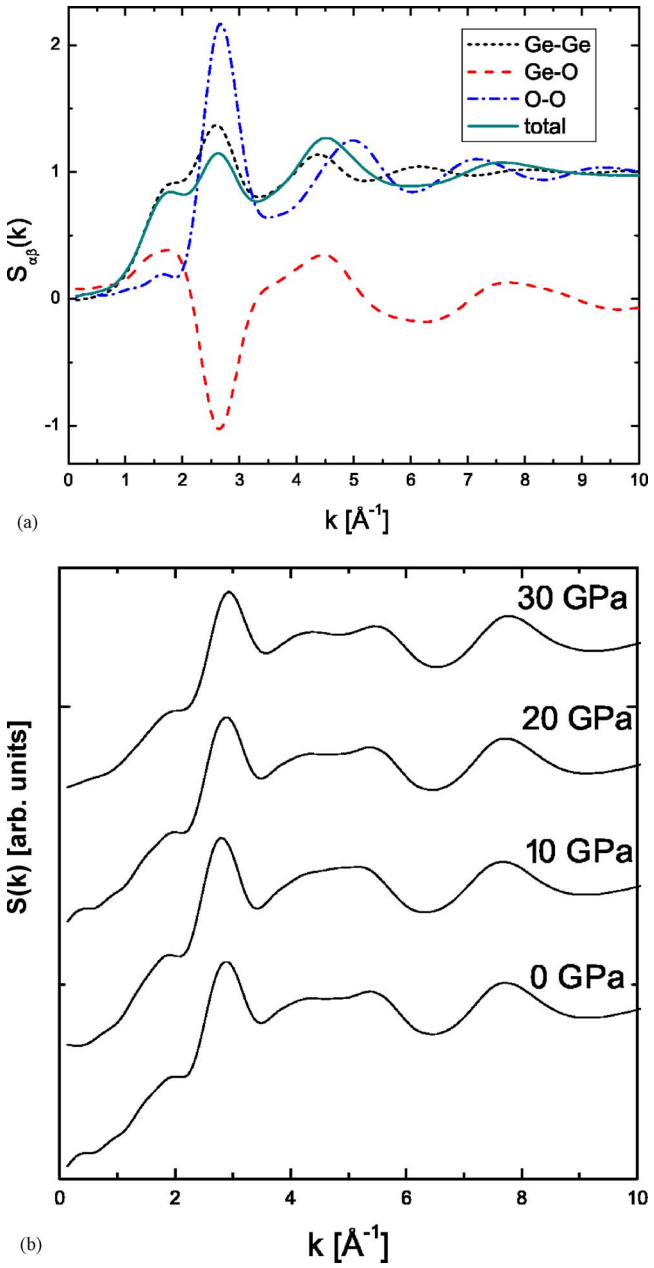

FIG. 10. (Color online) (a) Partial structure factors for vitreous GeO_2 at 300 K, 0.1 MPa. (b) Total structure factor at various pressures.

first-principles calculations, are in excellent agreement.[39] Comparing with experimental results[40] (1.54, 2.6, 4.5 Å^{-1}), we can associate these peaks with intermediate-range order, chemical short-range order, and topological short-range order, respectively. That is the third peak which arises from Ge-Ge, Ge-O, and O-O correlations, expresses GeO_4 tetrahedra in real space while the first two are responsible for real space correlations beyond correlations beyond ~3 Å.

High-pressure simulations were carried out at 300 and 1200 K and our results, shown in Figs. 11(a) and 11(b), display that the transition to the denser phase of the glass is gradual, without any discernible volume discontinuities. At 300 K, on release of pressure, GeO_2 continuously transforms back to a lower-density phase, while retaining a higher den-

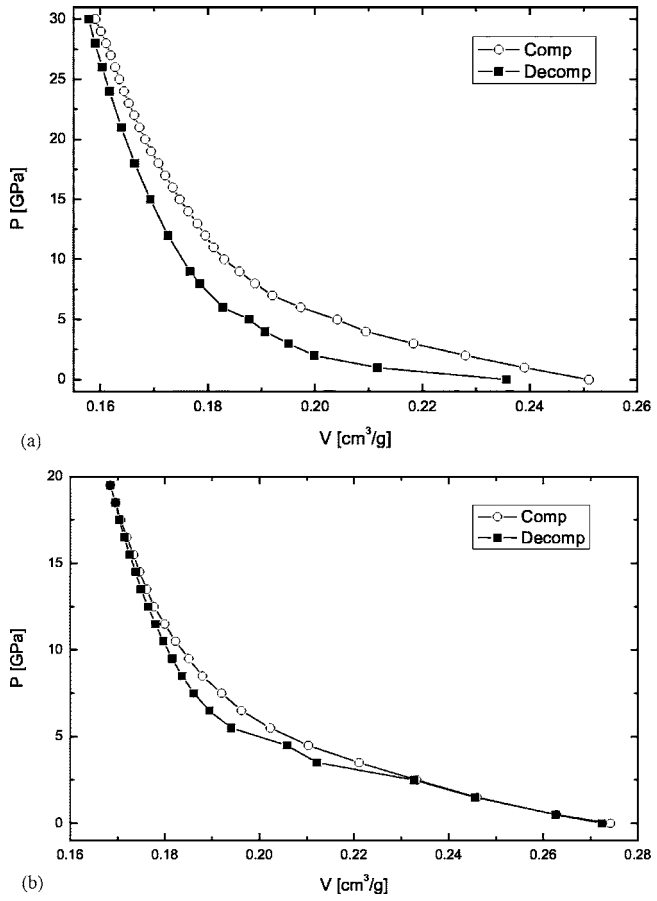

FIG. 11. Variation of volume with pressure in the vitreous GeO_2 at (a) 300 and (b) 1200 K.

sity compared to the values under compression. On complete unloading of the pressure, the retrieved glass remained about 6% denser, in qualitative agreement with the simulations by Micoulaut. However, at 1200 K, density differences between compression and decompression are somewhat less than at 300 K. At less than ~2 GPa, the *PV* behavior becomes es-

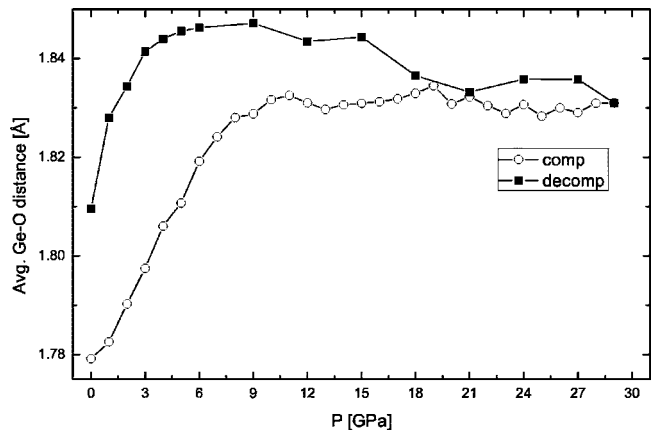

FIG. 12. Variation of Ge-O bond length with pressure during compression and decompression for the simulation of glass at 300 K.

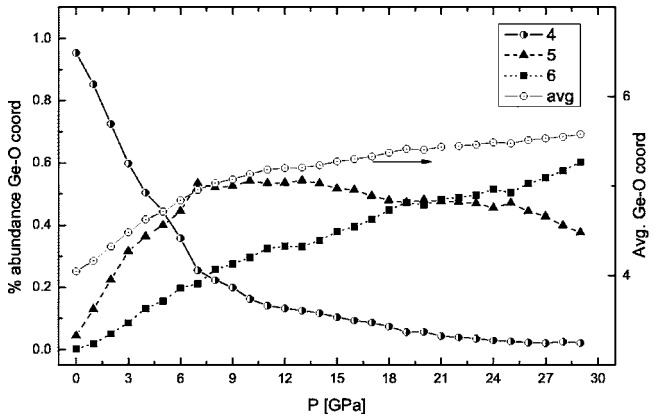

FIG. 13. Variation of fractional abundance of Ge-O coordination with pressure for vitreous GeO_2 at 300 K.

sentially identical to the compression cycle. Our results also show that at ~5 GPa, the structure relaxes somewhat discontinuously as shown in Fig. 11.

Figures 12 and 13 show the variations of Ge-O bond length and coordination with pressure. The Ge-O bond length increases gradually upon compression from 1.78 to 1.83 Å between 0 and 10 GPa. These results are slightly different from the earlier MD results of Micoulaut which showed that the Ge-O bond distance remains constant (1.72 Å) upto ~9 GPa and then increases to 1.79 Å up to 30 GPa. Upon decompression it follows a different path in qualitative agreement with the experimental results of Itie *et al.*,[1] although the bond lengths are slightly different. Also, our simulations show that even up to ~30 GPa, the state is not fully octahedrally connected as also observed in earlier MD studies.[28] This is at variance with the conclusions derived from the experiments that in amorphous germania Ge-O coordination becomes 6 at less than 15 GPa. One of the key results of our simulations is that we find a large number of Ge atoms (~50% at ~7 GPa) are coordinated to five oxygen atoms (Fig. 13). However, we do not find the existence of a plateau at 5 coordination, as claimed in recent experimental measurements by Guthrie *et al.*[13] In addition,

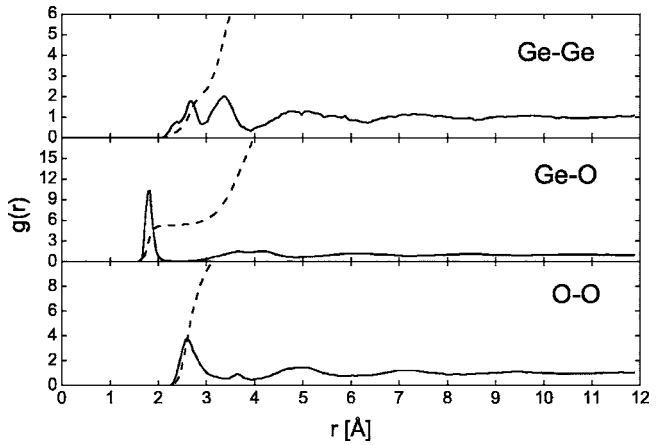

FIG. 14. Partial radial distribution functions for the simulation cell at 300 K and 15 GPa. Dotted line represents the running coordination number.

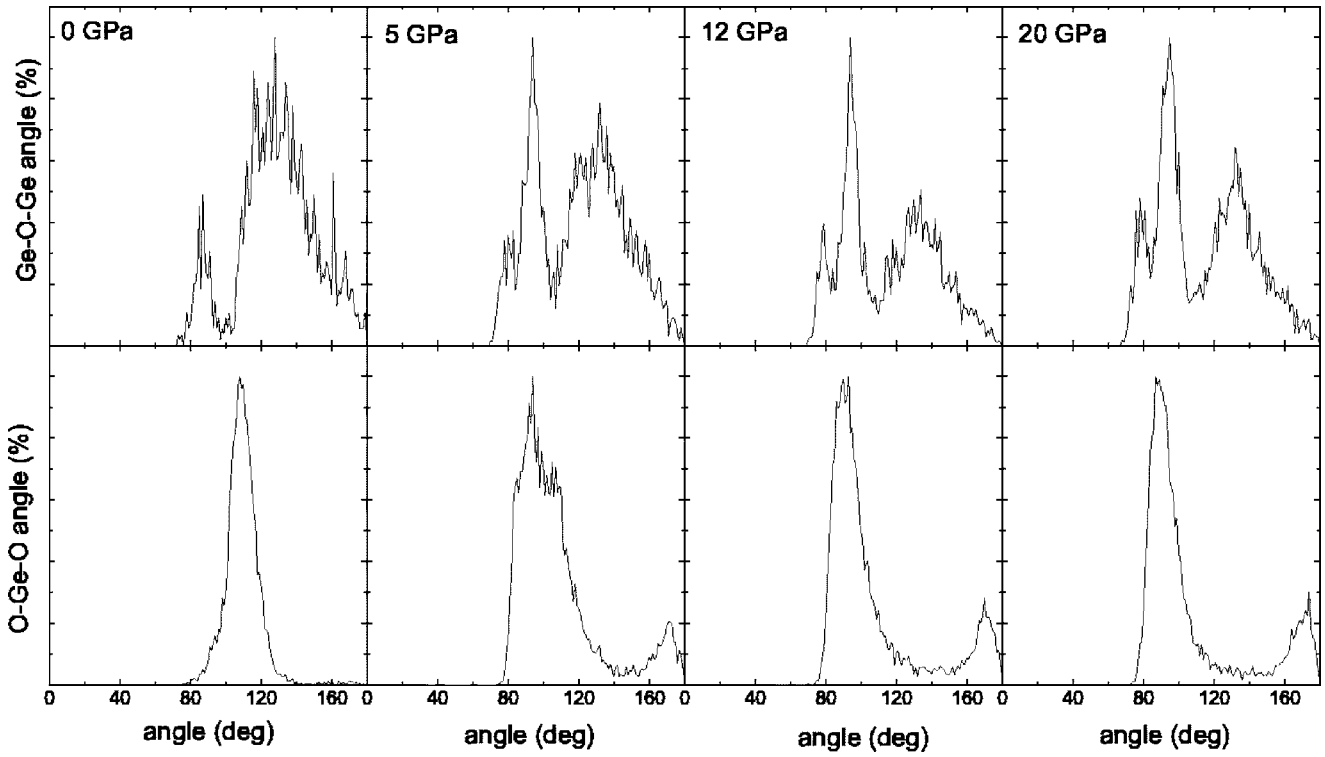

FIG. 15. Variation of Ge-O-Ge and O-Ge-O angle distribution with pressure for vitreous GeO_2.

we should also point out that earlier MD simulations on vitreous GeO_2 did not investigate the relevance and abundance of pentacoordinated states. To evaluate whether the experimental observations could be explained in terms of the nonhydrostatic stresses, we repeated the simulations with nonhydrostatic stresses. For this, the stress along one direction was kept about 1 GPa higher that in the other directions. Although the number of five-coordinated Ge ions remains almost constant over a wider range of pressure, the average coordination showed a similar behavior as under hydrostatic pressures. Unlike the earlier computations,[13] our simulations do show the coexistence of four- and six-coordinated Ge atoms in addition to the five-coordinated atoms. The computed variation of total coordination shows that there is no unambiguous plateau in the average coordination number even though the rate of coordination increase is rather small. The monotonic increase in the average Ge-O coordination with pressure, derived from simulations employing different interaction potentials, suggests that the interpretation of the results in terms of a pure pentahedral state[13] needs a fresh look.

From the pair distribution functions plotted in Fig. 14, we can see that at 15 GPa the first Ge-Ge peak splits into two peaks, located at 2.67 and 3.35 Å. Shorter Ge-Ge distances correspond to octahedral structure, suggesting that two Ge sites now exist corresponding to the tetrahedral and octahedral bonding,[25] as modeled in Ref. 1. Figure 15 confirms the growing abundance of the O-Ge-O angle at 90° and 170°, suggesting a reasonable population growth of octahedra. The interpolyhedral Ge-O-Ge angle distribution at 300 K shows a small peak at 85° ascribable to edge-shared tetrahedra. On increasing the pressure, another sharp peak develops around 90° which is likely to be due to edge-shared octahedra, reaffirming it to be a mixed coordinated state.

This section demonstrates that our results are broadly in agreement with that those of Itie *et al.* while in disagreement with those of Guthrie *et al.* Moreover, our simulation also shows that the results of Guthrie *et al.* are not easy to explain even in the presence of small deviatoric stresses. This suggests that the experimental conditions of observability of a five-coordination plateau should be better defined.

D. High-pressure study of liquid GeO_2

It was established in Sec. III A that GeO_2 melts beyond 1500 K at 0.1 MPa. In this section we present the results of

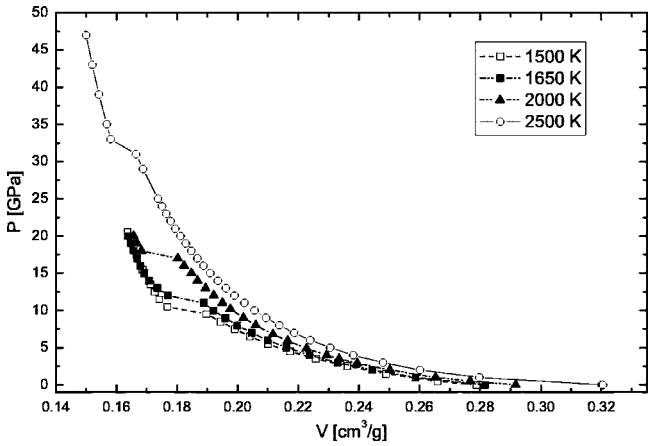

FIG. 16. Variation of the volume of GeO_2 on increase of pressure at 1500, 1650, 2000, and 2500 K.

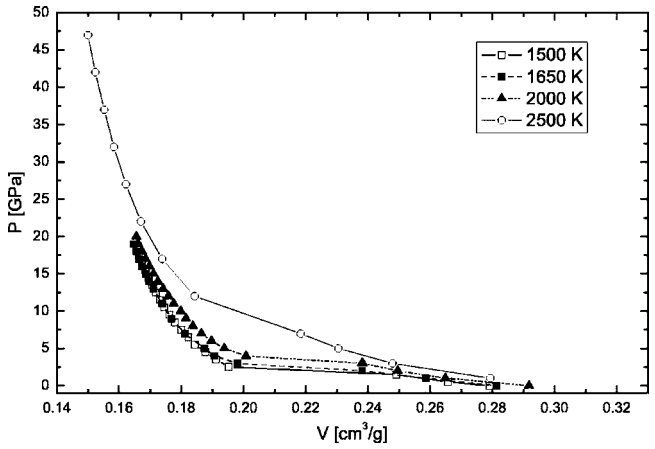

FIG. 17. Variation of volume of GeO_2 on unloading the pressure at 1500, 1650, 2000, and 2500 K.

our simulations at temperatures $\geqslant$1500 K. The computed P-V behavior at various temperatures is shown in Fig. 16. These results show that the initially molten phase shows a volume discontinuity on increase of pressure, at 9.5 GPa for the simulation at 1500 K, 11 GPa for 1650 K, 17 GPa for 2000 K, and 31 GPa for 2500 K. The observed volume collapse implies a first-order structural phase transition. The reversibility of the phase transition is implied by the results shown in Fig. 17, which shows the variation of the volume on release of pressure. Of course, there is a large hysteresis and the GeO_2 returns to the lower-density phase at 7, 3, 2, and 1.5 GPa for 2500, 2000, 1650, and 1500 K respectively.

Apart from the differences in the transition pressures, changes observed were similar at 1500, 1650, 2000, and 2500 K; hence we present here the detailed analysis of the changes at 1650 K only.

The low-density phase of the liquid at 1650 K, having a density of 3.55 g/cm^3, was composed of randomly connected GeO_4 tetrahedra with average Ge-O bond length of 1.81 Å. Figure 18 shows the computed partial structure factors at 1650 K and 0.1 MPa, with peaks at 1.64, 2.54, and 4.35 Å^{-1}. Peaks at larger k correspond to correlations at shorter r and the third peak can be associated with the short-range order of the GeO_4 tetrahedron.

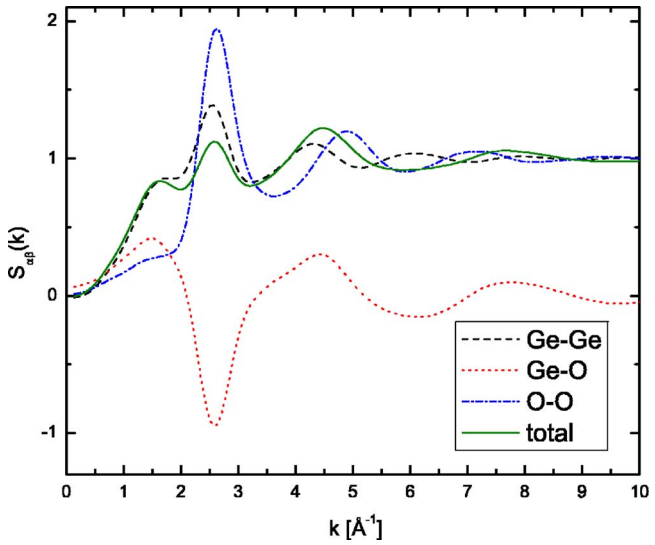

FIG. 18. (Color online) Computed partial and total structure factors of liquid GeO_2 at 1650 K and 0.1 MPa.

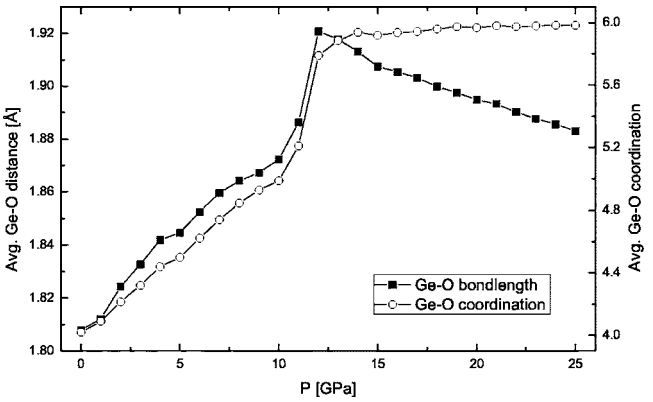

FIG. 19. Variation of Ge-O distance and coordination with pressure at 1650 K.

As mentioned in Sec. I, the recent experiments on liquid alkali-metal germanates, showed that the deduced Ge-O bond length reached a maximum (1.91 Å at 3–4 GPa) and gradually reduced thereafter. Because the observed distances were comparable to the rutile type crystalline GeO_2 at 1273 K, the x-ray absorption near-edge spectra in this pressure region were interpreted as an indication of sixfold coordination. Our results shown in Figs. 19 and 20 qualitatively agree with this conclusion. The Ge-O distance increases to a maximum of 1.92 Å at the transition pressure at which the Ge-O coordination becomes 6. We also see that the system goes through an intermediate phase where a large percentage ($\sim$50%) of Ge atoms are five coordinated. On release of pressure the initial Ge-O bond length and coordination are retrieved.

The distribution of Ge-O-Ge and O-Ge-O angles is shown in Fig. 21. At ambient conditions, the first peak at $\sim$85° in the Ge-O-Ge angle distribution is due to the edge-shared tetrahedra. On increasing the pressure this peak vanishes and a sharp peak emerges at 90°, representing the edge-shared octahedra. Computation of the network connectivity con-

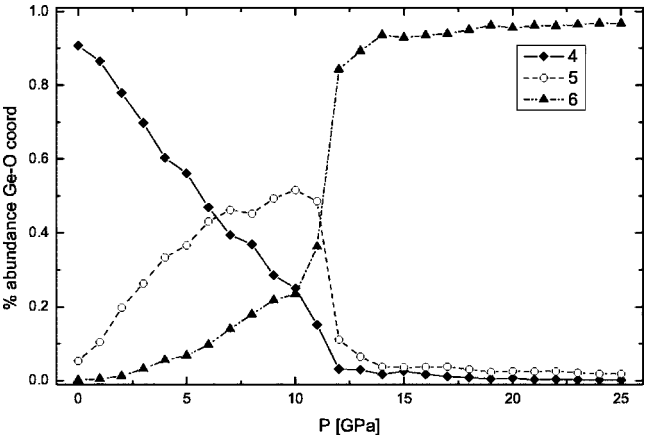

FIG. 20. Variation of fractional abundance of Ge-O coordination with pressure at 1650 K.

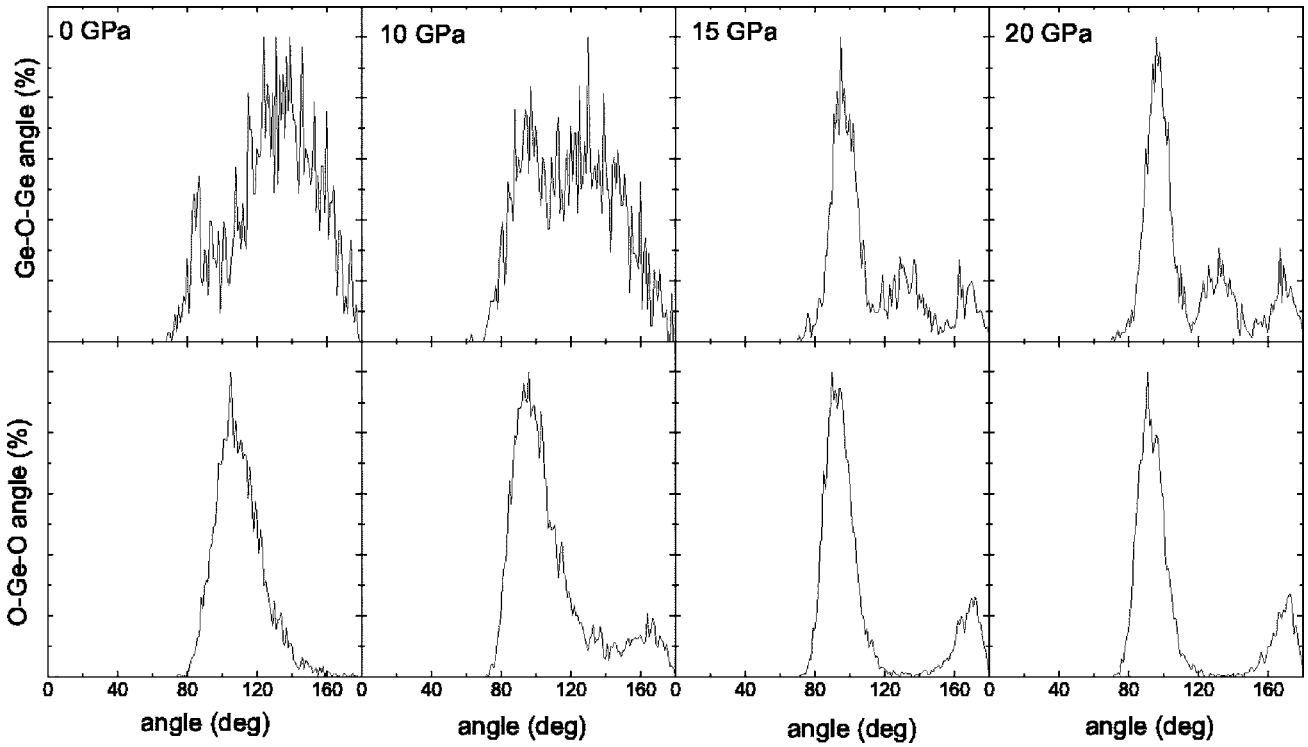

FIG. 21. Variation of Ge-O-Ge and O-Ge-O angle distribution with pressure at 1650 K.

firms that the high-pressure denser phase consists primarily of edge-shared octahedra. Variation of the structure factor with pressure is depicted in Fig. 22. We should note that at higher pressure $S(q)$ shows more peaks, implying larger intermediate-range order in the high-pressure phase. This feature is also supported by the bond angle distributions shown in Fig. 21.

To determine whether the high-pressure phase is a disordered solid or liquid, we evaluated the relative thermal displacements as well as the elasticity of the cell deformation. At the same temperature, the atomic displacements may be more than an order of magnitude larger in the liquid than in the solid phase. Also, the liquid phase should deform plastically under the action of a shear force whereas a solid regains the original shape upon the removal of shear stress. Calculations of mean square displacement $\langle r^2 \rangle$ showed that in the high-pressure phase (at 15 GPa, 1650 K) the $\langle r^2 \rangle$ is about ten times less ($\sim$0.17 Å) than the corresponding value at ambient pressure ($\sim$1.9 Å), suggesting that the high-pressure phase may be solidlike. For the deformational response, the time evolution of the MD cell, initially deformed as under the shear, was investigated to determine whether it equilibrates to the undeformed state. For this, the simulation cell (at 15 GPa, 1650 K and 33 GPa, 2500 K) was deformed by a small amount[36] and then the cell was equilibrated under no-stress conditions. It was observed that for the high-density phase the cell returned to the form with 90° angle. At ambient pressure such a reversal was not observed. These results suggest that the high-pressure phase is probably an amorphous solidlike phase.

Since the earlier computer simulations of liquid GeO_2 were carried out at higher densities compared to ours, the present results suggest that the high-pressure phase in those simulations may also correspond to a glass phase rather than a liquid phase. Our results also suggest a fresh look into the interpretation of the experimental observation in terms of low-density to high-density liquid-liquid transformations. In particular, the denser high-pressure phase needs to be better characterized.

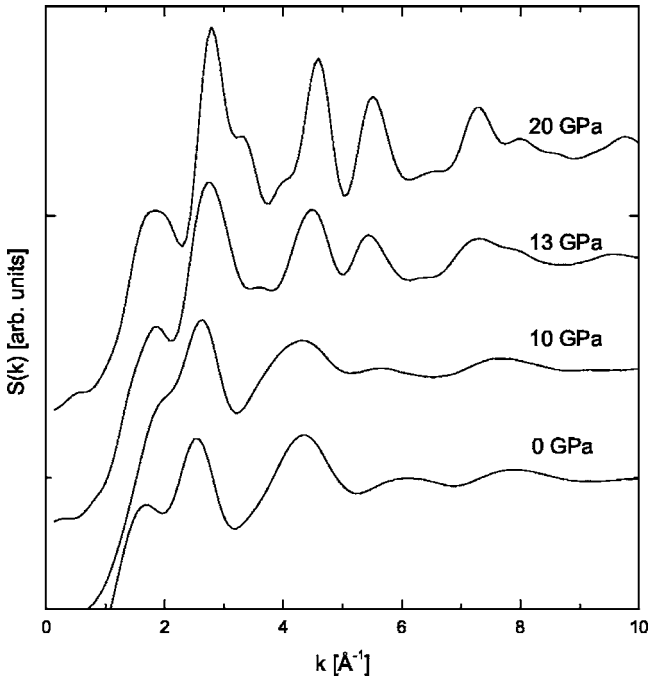

FIG. 22. Variation of structure factor with pressure at 1650 K.

In addition, our calculations show that the high-pressure glasslike phase obtained by compressing the GeO_2 melt is considerably different from the high-pressure glass obtained by pressurizing solid vitreous GeO_2. The former is fully six coordinated whereas in the latter the Ge-O coordination is a mixture of 5 and 6. In addition, the comparison of the computed partial structure factors implies that the high-pressure glasslike phase obtained from the melt has more intermediate-range order than the state from initial vitreous GeO_2. Obviously these differences arise from the ease of atomic and molecular adjustments possible due to higher atomic mobility in the liquid phase prior to the transformation to the solidlike phase than in the solid vitreous state.

IV. CONCLUSIONS

To summarize, we have studied the high-pressure, high-temperature behavior of α-GeO_2, GeO_2 glass, and liquid GeO_2 with the help of classical molecular dynamics simulations. At ambient pressure, these simulations reproduce the α-β transformation and the melting of GeO_2. The calculations on α-GeO_2 indicate that at 9 GPa it transforms to a monoclinic phase having mixed Ge-O coordination of 4, 5, and 6. These simulations suggest that the EXAFS results[1] should be analyzed in terms of all three coordination states rather than only in terms of four- and six-coordinated states. In addition, our simulations on vitreous GeO_2 also display a smooth variation of the mixed coordinated state of 4, 5, and 6 and do not support the stability of the pentahedral state over a pressure range of 6–10 GPa, as reported by Guthrie *et al.* We have also shown that at high pressures liquid GeO_2 undergoes a first-order phase transition to a six-coordinated amorphous solidlike phase, suggesting a fresh look into the experimental results claiming liquid-liquid transformations at high pressures.

ACKNOWLEDGMENTS

The authors wish to thank H. K. Poswal and K. Rajesh for useful discussions.

[1] J. P. Itie, A. Polian, G. Calas, J. Petiau, A. Fontaine, and H. Tolentino, Phys. Rev. Lett. **63**, 398 (1989).
[2] C. H. Polsky, K. H. Smith, and G. H. Wolf, J. Non-Cryst. Solids **248**, 259 (1999).
[3] V. V. Brazhkin and A. G. Lyapin, J. Phys.: Condens. Matter **15**, 6059 (2003).
[4] R. D. Oeffner and S. R. Elliot, Phys. Rev. B **58**, 14791 (1998).
[5] S. Ono, T. Tsuchiya, K. Hirose, and Y. Ohishi, Phys. Rev. B **68**, 014103 (2003).
[6] J. Haines, J. M. Léger, and C. Chateau, Phys. Rev. B **61**, 8701 (2000).
[7] V. V. Brazhkin, A. G. Lyapin, R. N. Voloshin, S. V. Popova, E. V. Tar'yanin, and N. F. Borovikov, Phys. Rev. Lett. **90**, 145503 (2003).
[8] N. Suresh, G. Jyoti, S. C. Sikka, and S. C. Sabharwal, J. Appl. Phys. **76**, 1530 (1994); M. S. Somayazulu, Nandini Garg, Surinder M. Sharma, and S. K. Sikka, Pramana **43**, 1 (1994); S. Kawasaki, O. Ohtaka, and T. Yamanaka, Phys. Chem. Miner. **20**, 531 (1994).
[9] M. Grimsditch, R. Bhadra, and Y. Meng, Phys. Rev. B **38**, 7836 (1988).
[10] C. Meade, R. J. Hemley, and H. K. Mao, Phys. Rev. Lett. **69**, 1387 (1992).
[11] D. J. Durben and G. H. Wolf, Phys. Rev. B **43**, 2355 (1991).
[12] C. E. Stone, A. C. Hannon, T. Ishihara, N. Kitamura, Y. Shirakawa, R. N. Sinclair, N. Umesaki, and A. C. Write, J. Non-Cryst. Solids **293-295**, 769 (2001).
[13] M. Guthrie, C. A. Tulk, C. J. Benmore, J. Xu, J. L. Yarger, D. D. Klug, J. S. Tse, H. Mao, and R. J. Hemley, Phys. Rev. Lett. **93**, 115502 (2004).
[14] H. Tanaka, Phys. Rev. E **62**, 6968 (2000).
[15] M. Togaya, Phys. Rev. Lett. **79**, 2474 (1997).
[16] Y. Katayama, T. Mizhutani, W. Utsumi, O. Shimomura, M. Yamakata, and K. Funakoshi, Nature (London) **403**, 170 (2000).
[17] O. Mishima and H. E. Stanley, Nature (London) **396**, 329 (1998).
[18] I. Saika-Voivod, F. Sciortino, and P. H. Poole, Phys. Rev. E **63**, 011202 (2000).
[19] C. A. Angell, S. Borick, and M. Grabow, J. Non-Cryst. Solids **205-207**, 463 (1996).
[20] P. H. Poole, F. Sciortino, U. Essmann, and H. E. Stanley, Nature (London) **360**, 324 (1992).
[21] J. N. Glosli and F. H. Ree, Phys. Rev. Lett. **82**, 4659 (1999).
[22] P. H. Poole, T. Grande, C. A. Angell, and P. F. McMillan, Science **275**, 322 (1997).
[23] O. Ohtaka, H. Arima, H. Fukui, W. Utsumi, Y. Katayama, and A. Yoshiasa, Phys. Rev. Lett. **92**, 155506 (2004).
[24] T. Tsuchiya, T. Yamanaka, and M. Matsui, Phys. Chem. Miner. **25**, 94 (1998).
[25] G. Gutierréz and J. Rogan, Phys. Rev. E **69**, 031201 (2004).
[26] T. Tsuchiya, T. Yamanaka, and M. Matsui, Phys. Chem. Miner. **27**, 149 (2000).
[27] T. Varma and S. M. Sharma, in *Proceedings of DAE Solid State Physics Symposium*, edited by R. Mukhopadhyay, B. K. Godwal, and S. M. Yusu (University Press, Hyderabad, 2000), 42, p. 176.
[28] M. Micoulaut, J. Phys.: Condens. Matter **16**, L131 (2004).
[29] K. Trachenko, M. T. Dove, V. Brazhkin, and F. S. El'kin, Phys. Rev. Lett. **93**, 135502 (2004).
[30] W. Smith, M. Leslie, and T. R. Forester, computer code DL_POLY_2.14 (CCLRC, Daresbury Laboratory, Daresbury, England, 2003).
[31] T. Yamanaka and K. Ogata, J. Appl. Crystallogr. **24**, 111 (1991).
[32] S. Melchionna, G. Ciccotti, and B. L. Holian, Mol. Phys. **78**, 533 (1993).
[33] D. M. Hatch and S. Ghose, Phys. Chem. Miner. **17**, 554 (1991).
[34] P. H. Berens and K. R. Wilson, J. Chem. Phys. **74**, 4872 (1981).
[35] S. Tsuneyuki, H. Akoi, and M. Tsukada, Phys. Rev. Lett. **64**, 776 (1990).
[36] The simulation cell is deformed through a small angle, such that the angle between *c* and *a* axes of the cell is reduced by 2°–5°

from the initial value of 90°. This is equivalent to applying a shear stress $-\sigma_{xz}$. In addition to the observed reduction in $\langle r^2 \rangle$, this may be a useful procedure to evaluate solidification. However, we should note here that the issue of characterizing a glass or a supercooled liquid in terms of stress relaxation times is not unambiguous [C. A. Angell, Science **267**, 1924 (1995); R. Bohmer, K. L. Nagai, C. A. Angell, and D. J. Plazek, J. Chem. Phys. **99**, 4201, (1993)]. Therefore, we tend to term the state with shear rigidity as "solidlike" or "glasslike."

[37] M. S. Somayazulu, Surinder M. Sharma, Nandini Garg, S. L. Chaplot, and S. K. Sikka, J. Phys.: Condens. Matter **5**, 6345 (1993).

[38] We should point out that the simulations carried out with different sizes of the MD cells show substantially different degree of disorder in the dense high-pressure phase. Simulation with a MD cell made of $9 \times 9 \times 6$ crystallographic unit cells, showed large disordered regions, whereas for the $8 \times 8 \times 4$ the structure was mostly ordered, except at the corners, and for $4 \times 4 \times 2$ it was fully ordered. A careful look into the structures shows that the high-pressure phase is related to the initial α phase through cell doubling along the a and b axes. This could explain why the MD cell having $9 \times 9 \times 6$ unit cells shows considerable disorder. It is probable that the earlier simulations (Ref. 24) which concluded amorphization of GeO_2 at high pressures may have an incompatible number of α-quartz unit cells.

[39] Luigi Giacomazzi, P. Umari, and Alfredo Pasquarello, Phys. Rev. Lett. **95**, 075505 (2005).

[40] D. L. Price, M.-L. Saboungi, and A. C. Barnes, Phys. Rev. Lett. **81**, 3207 (1998).